ARTICLE IN PRESS

Ceramics International xxx (xxxx) xxx–xxx

Contents lists available at ScienceDirect

Ceramics International

journal homepage: www.elsevier.com/locate/ceramint

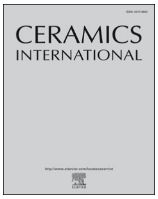

A novel “plane-line-plane” nanostructure of the sandwich-like CNTs@SnO_2/$Ti_3C_2T_x$ 3D nanocomposite as a promising anode for lithium-ion batteries

Zhichao Liu, Ruisong Guo*, Mei Zheng, Fuyun Li, Baoyu Wang, Tingting Li, Yani Luo

Key Laboratory of Advanced Ceramics and Machining Technology of Ministry of Education, School of Materials Science and Engineering, Tianjin University, Tianjin 300354, China

ARTICLE INFO

Keywords:
$Ti_3C_2T_x$
SnO_2
CNTs
Lithium-ion battery
Nanocomposite

ABSTRACT

As one of the novel two-dimensional metal carbides, $Ti_3C_2T_x$ has received intense attention for lithium-ion batteries. However, $Ti_3C_2T_x$ has low intrinsic capacity due to the fact that the surface functionalization of F and OH blocks Li ion transport. Herein a novel “plane-line-plane” three-dimensional (3D) nanostructure is designed and created by introducing the carbon nanotubes (CNTs) and SnO_2 nanoparticles to $Ti_3C_2T_x$ via a simple hydrothermal method. Due to the capacitance contribution of SnO_2 as well as the buffer role of CNTs, the as-fabricated sandwich-like CNTs@SnO_2/$Ti_3C_2T_x$ nanocomposite shows high lithium ion storage capabilities, excellent rate capability and superior cyclic stability. The galvanostatic electrochemical measurements indicate that the nanocomposite exhibits a superior capacity of 604.1 mAh g^{-1} at 0.05 A g^{-1}, which is higher than that of raw $Ti_3C_2T_x$ (404.9 mAh g^{-1}). Even at 3 A g^{-1}, it retains a stable capacity (91.7 mAh g^{-1}). This capacity is almost 5.6 times higher than that of $Ti_3C_2T_x$ (16.6 mAh g^{-1}) and 58 times higher than that of SnO_2/$Ti_3C_2T_x$ (1.6 mAh g^{-1}). Additionally, the capacity of CNTs@SnO_2/$Ti_3C_2T_x$ for the 50th cycle is 180.1 mAh g^{-1} at 0.5 A g^{-1}, also higher than that of $Ti_3C_2T_x$ (117.2 mAh g^{-1}) and SnO_2/$Ti_3C_2T_x$ (65.8 mAh g^{-1}), respectively.

1. Introduction

The fast depletion of traditional energy and a serious environmental concerns have generated more attention to develop advanced renewable energy sources [1–3]. To date, due to high energy density, high rate capability and long cycle life, lithium ion batteries (LIBs) as a high-performance energy storage device have been widely used for portable electronics, electric vehicles, etc. To enhance these properties, numerous types of new electrode materials with high capacity, long-term cyclability and superior rate capability have aroused extensive attention for the future generation of energy storage [2–7].

As one of the most important two-dimensional (2D)-layered nanomaterials which exhibit large exposed surfaces and excellent electronic transport properties, graphene has attracted significant interests in recent years [2,8–10]. It is a two-dimensional one-atom-thick sheet of sp^2 bonds carbon atoms and is widely used in numerous areas due to its unique ultra-thin thickness and excellent electrical, thermal and mechanical properties. Nevertheless, the single-element 2D material only with carbon might limit its application as anode in LIBs because of the unadjustable component element. Encouragingly, the majority of the 2D materials contain two or more elements, such as oxides, transition metal dichalcogenides, clays, etc. [4–6,11,12] These 2D materials with more than one elements can exist in various forms: solid solutions, ordered phases, etc. Additionally, a random arrangement of two or more different elements leads to the multiformity of compound composition, thus more excellent properties can be obtained.

Recently, a new group of transition metal carbides, carbonitrides and nitrides (MXenes) have been among the latest additions to the family of 2D materials [6,7,13]. They are synthesized by extracting the “A” element from the MAX phases. Their general formula is $M_{n+1}X_nT_x$ (n = 1–3), where “M” is an early transition metal (M = Ti, Sr, V, Cr, Ta, Nb, Zr, Mo and Hf), T_x stands for a functionalization group of hydroxyl, oxygen or fluorine (depending on aqueous HF etching process) and “X” denotes C or/and N [14–19].

Compared with the conventional lithium ion anode material, MXenes have wide chemical and structural variety, which makes them competitive with other 2D material. A lithium ion capacity in excess of 750 mAh g^{-1} was achieved for CNTs/MXene by optimization of the electrode architecture. Beyond, the delaminated MXene “paper” showed a capacity of 410 mAh g^{-1} at a 1 C cycling rate (~0.4 A g^{-1}). Meanwhile, MXenes have shown an excellent capability to handle high cycling rates. For example, a reversible capacity of 110 mAh g^{-1} was obtained for delaminated MXene anode at 36 C (~14.8 A g^{-1}) after 200 cycles [6,7,18,19].

---

* Corresponding author.
E-mail address: rsguo@tju.edu.cn (R. Guo).

https://doi.org/10.1016/j.ceramint.2018.03.256
Received 21 February 2018; Received in revised form 27 March 2018; Accepted 28 March 2018

Please cite this article as: Liu, Z., Ceramics International (2018), https://doi.org/10.1016/j.ceramint.2018.03.256

Among the above-mentioned MXenes, $Ti_3C_2T_x$ has been the first MXene reported since 2011 [13]. Density functional theory (DFT) calculations predict that the corresponding theoretical specific capacity of Ti_3C_2, $Ti_3C_2F_2$ and $Ti_3C_2(OH)_2$ can reach 320, 130, and 67 mAh g^{-1}, respectively [20,21]. Although $Ti_3C_2T_x$ has good electrical conductivity and fast Li^+ diffusion, the capacity of $Ti_3C_2T_x$ anode cannot meet the demand for high capacity batteries, which limits its application as lithium electrode materials [22–24].

Transition metal oxides have been attractive anodes due to their high theoretical capacities, low costs and environmental benignity [5,25–29]. Among them, tin dioxide (SnO_2) has been regarded as a promising anode material for LIBs on account of its high theoretical specific capacity of 782 mAh g^{-1} [29]. However, SnO_2 has poor rate capability and large volume change which renders rapid capacity loss during charge/discharge processes [5,29]. To tackle these problems, the most useful approach is to reduce SnO_2 size to the nanoscale region and composite SnO_2 with different carbonaceous supports. Meanwhile, many studies have proved that SnO_2 as an outstanding chemical modifier could greatly improve the electrochemical performance of SnO_2-based nanocomposites [29–33].

The Li diffusion barrier is calculated for SnO_2. The energy barriers of paths x and y are 2.23 and 0.49 eV, respectively. The path x is equivalent to path z in the square symmetry of the SnO_2 structure. It means that path y is the main Li diffusion pathway [34]. In addition, theoretical studies have indicated that the Li diffusion within the graphite interlayers needs to overcome a relatively high energy barrier of 0.3 eV. Meanwhile, $Ti_3C_2T_x$ monolayer exhibits a much lower barrier for Li diffusion (the predicted diffusion barrier is 0.07 eV for Ti_3C_2) [13,18]. This means that $Ti_3C_2T_x$ monolayer can exhibit faster Li transport and higher charge/discharge rates. Unfortunately, its specific capacity (Ti_3C_2 (320 mAh g^{-1}), $Ti_3C_2F_2$ (130 mAh g^{-1}) and $Ti_3C_2(OH)_2$ (67 mAh g^{-1})) is less advantageous than that of graphite (372 mAh g^{-1}) [20,21]. Based on this, we have attempted to fabricate SnO_2 nanoparticle-modified $Ti_3C_2T_x$ nanocomposite ($SnO_2/Ti_3C_2T_x$) via a simple hydrothermal process. Meanwhile, a carbonaceous support (carbon nanotubes, CNTs) is introduced into the $SnO_2/Ti_3C_2T_x$ nanocomposite for the first time as a type of conductive additive to construct a three-dimensional (3D) crosslinked network structure. For this 3D nanocomposite (CNTs@$SnO_2/Ti_3C_2T_x$), $Ti_3C_2T_x$ acts as the 2D support network to enhance the electronic transport properties and provides part of the capacity. SnO_2 supplies a higher reversible capacity. CNTs, as a 1-D material, not only buffer the volume change of SnO_2 nanoparticles during charge-discharge processes, but also strengthens the electrical conductivity of the nanocomposite. Hence, this kind of 3D network structure turns the original "plane-plane" 2D structures of $Ti_3C_2T_x$ to a novel "plane-line-plane" 3D conducting mode. It can provide lower charge transfer resistance and higher diffusion coefficient of lithium ions for the CNTs@$SnO_2/Ti_3C_2T_x$ nanocomposite. The designed CNTs@$SnO_2/Ti_3C_2T_x$ nanocomposite can be expected to be used as anode material and exhibit excellent lithium-storage performance, superior cycling stability and rate capability. Fig. 1 schematically illustrates the typical 3D nanostructure. Firstly, 2D-layered $Ti_3C_2T_x$ is formed by wet HF treatment of inexpensive Ti_3AlC_2, then SnO_2 nanoparticles branch on $Ti_3C_2T_x$ matrix. Whereafter the CNTs is deposited on $SnO_2/Ti_3C_2T_x$ nanocomposite.

2. Experimental section

All chemical reagents were of analytical reagent grade and used without further purification. And all the aqueous solutions were prepared using distilled water.

Ti_3AlC_2 powders (> 98 wt% purity, −325 mesh) were supplied by the Ningbo Institute of Industrial Technology, Chinese Academy of Sciences, China. 1 g Ti_3AlC_2 particles were immersed into 20 mL 49–51% HF solution at room temperature for 24 h to exfoliate the Al layers. Then the resulting powders were repeatedly rinsed by distilled water until pH value of the solution reached ∼ 5. The obtained sediment was allowed to desiccate under vacuum at 90 °C for 24 h [9]. A rudimentary yield by mass was 88%.

CNTs were synthesized by the chemical vapor deposition (CVD) method and purified by homogenous H_2O_2 at room temperature [35,36]. The CNTs@$SnO_2/Ti_3C_2T_x$ 3D nanocomposite was synthesized by a facile hydrothermal method. 0.5 g $Ti_3C_2T_x$ powders were dispersed into a 0.5 M $SnCl_2{\cdot}4H_2O$ solution (20 mL) and ultrasonic for 0.5 h. Then the suspension was stirred for 2 h before transferred into a 50 mL Teflon-lined autoclave and heated at 130 °C for 5 h. After cooling down to room temperature naturally, the resulting precipitate was washed by distilled water for 3 times. The sample ($SnO_2/Ti_3C_2T_x$) was dried at 80 °C for 12 h. Finally, 0.055 g of the as-prepared CNTs (School of Materials Science and Engineering, Tianjin University, China) was dispersed into 20 mL of $SnO_2/Ti_3C_2T_x$ (0.5 g) suspension under ultrasonication for 0.5 h. Then the suspension was stirred for another 4 h. Afterwards, the mixture was transferred into a 50 mL Teflon-lined autoclave. The suspension was added up to 75% of the total volume and maintained at 130 °C for 6 h. Whereafter, the precipitate was obtained after the Teflon-lined autoclave was naturally cooled down to room temperature. The products were rinsed with distilled water for 5 times, and finally dried at 80 °C for 12 h.

X-ray powder diffraction (XRD, Cu Kα radiation (λ = 0.154059 nm), Rigaku D/max-2500) was used to analyze the crystalline structure of the samples. Field emission scanning electron microscope (FE-SEM: Hitachi, S-4800) was applied to observe the morphology of the samples. High resolution transmission electron microscopy (HRTEM, Philips, Tecnai G2 F20) equipped with an energy dispersive X-ray spectroscopy detector (EDS) was assigned to observe the microstructure of the samples and investigate the element distribution. The surface composition and chemical states of the specimens were investigated using X-ray photoelectron spectroscopy (XPS, ESCALAB 250Xi, PHI quanteda ii).

The electrochemical properties of anode materials ($Ti_3C_2T_x$, $SnO_2/Ti_3C_2T_x$ and CNTs@$SnO_2/Ti_3C_2T_x$) were measured using coin-type (CR2430) half cells. The anode slurry was fabricated by mixing the 80 wt% active materials ($Ti_3C_2T_x$, $SnO_2/Ti_3C_2T_x$ and CNTs@$SnO_2/Ti_3C_2T_x$), 10 wt% Super P carbon black and 10 wt% polyvinylidene fluoride (PVDF) in N-methyl-2-pyrrolidinone (NMP), then the slurry was homogeneously cast onto an Cu foil and subsequently dried in vacuum at 90 °C for 12 h. The thickness of the film is approximately 0.13 mm. The film was dried again at 80 °C for 1 h under vacuum and then cut into circular slices with diameter of 12 mm. Then the working electrode was assembled in an argon filled glove box with the use of Celgard 2400 as a seperator and metal Li foil as counter electrode. The electrolyte was 1 M $LiPF_6$ in a mixture of ethylene carbonate (EC) and dimethyl carbonate (DMC) (1:1 in volume). The typical loading of the active materials is in the range of 2–3 mg cm^{-2}, depending on the different active materials. All the cells were allowed to age for 24 h before testing. The galvanostatic charge/discharge tests were carried out using a Neware battery test system between 0.001 and 3.0 V at room temperature. The cyclic voltammetry (CV, Chenhua CHI660C Electrochemical Workstation) curves were obtained at a scan rate of 0.1 mV s^{-1} within 0.001–3.0 V. Electrochemical impedance spectroscopy (EIS) measurements were performed by a CHI660C electrochemical workstation in the frequency ranging from 0.1 Hz to 100 kHz with an amplitude of 5 mV.

3. Results and discussion

The as-prepared samples (Ti_3AlC_2, $Ti_3C_2T_x$, $SnO_2/Ti_3C_2T_x$ and CNTs@$SnO_2/Ti_3C_2T_x$) were characterized using X-ray diffraction (XRD) to examine the phase structures (Fig. 2). As depicted in Fig. 2a, the diffraction peaks of the raw material corresponded well to Ti_3AlC_2 (JCPDS No. 52–0875). The diffractogram of $Ti_3C_2T_x$ shows the specific (002), (006) and (110) peaks. Most surprisingly, the most intensive